Testing and Evaluation of Bridges

Evaluation of the John Coffee Memorial Bridge demonstrates inspection tools of the future

by Mohammad S. Khan

Built in 1964, the John Coffee Memorial Bridge (Fig. 1) is a nearly 1 mile (1.6 km) long bridge that carries Natchez Trace Parkway over the Tennessee River. The two-lane, 38-span, plate-girder bridge with concrete deck provides a direct route for travelers from Tennessee to Mississippi. While the bridge has exhibited deterioration in both the superstructure and substructure, it has not yet undergone any major rehabilitation. Because of its scale, inspection is challenging. In 2018, for example, a manual visual inspection of the piers required a snooper truck on the deck, traffic control, and a bucket boat on the river waters. A recent evaluation was conducted to select appropriate restoration methods, using robotic tools that enabled nondestructive evaluations (NDEs) without the need for traffic control. This article describes these tools and summarizes the evaluation.

Fig. 1: John Coffee Memorial Bridge

Background

Efforts are continually being made to improve the techniques used for bridge inspections, including the use of uncrewed aerial systems (UAS) and/or robotic crawlers. In 2015, the Minnesota Department of Transportation (MnDOT) conducted a demonstration project on the use of UAS in bridge safety inspections on four different bridges across the state.[1] It was concluded that the technology can be safely used in the field with a low risk to the public and inspection personnel. In Phase II of the MnDOT study, still image, video, and infrared cameras mounted on various UAS products were tested.[2] The researchers concluded that UAS used in conjunction with infrared (IR) sensors can be an effective way to detect concrete delamination, and it can be done without closing a bridge to traffic. While the researchers also concluded that measurements can be estimated from images, they noted that a UAS cannot replicate tactile functions such as sounding, measuring, and testing. A report published in 2018 by the Federal Highway Administration (FHWA) noted that transportation departments that have implemented UAS programs have found that UAS can save time and money as well as increase safety and efficiency.[3]

Many NDE technologies now used in the transportation industry have been previously used in other industries, including the medical and defense industries. Computed tomography and UAS are a few examples.

NDE applications include collecting, processing, and analyzing data; assessing the type and extent of deterioration; forecasting the remaining service life; and selecting remedial actions, including maintenance, repair, rehabilitation, or replacement. With the development of different asset management systems, including bridge and pavement management systems,[4,5] progress has been made in integrating the entire process of NDE application, starting from inspection and testing to selecting the remedial action. However, the process is still largely fragmented and compartmentalized.

Several NDE technologies have been incorporated on a robotic platform for the detection and monitoring of a variety of concrete deterioration mechanisms, resulting in a system, "Robotic Assisted Bridge Inspection Tool (RABIT™)."[6] RABIT includes electrical resistivity, impact echo, ultrasonic surface waves, ground-penetrating radar (GPR), and a panoramic camera. This system can monitor visible surface defects through the camera, and it can assess the likelihood of corrosion, delamination, and degradation through the other installed NDE techniques. Although RABIT allows tactile inspection of horizontal surfaces (for example, bridge decks), it cannot climb vertical surfaces (for example, piers and abutments). However, crawling robots equipped with NDE technologies have been developed to detect subsurface defects in girders, piers, and abutments; and a crawling robot equipped with GPR and a high-resolution imaging (HRI) camera has been used with limited success in the inspection and testing of a dam.[7] Further, a magnetic flux leakage (MFL) NDE system has been developed that can detect corrosion-induced damage in prestressed concrete girders under a bridge deck.[8] However, most crawling robots are unsuitable for inspection of vertical concrete surfaces.

John Coffee Memorial Bridge Assessment

NDE assessments of the subject bridge were recently conducted using state-of-the-art equipment, including a UAS and a crawling robot (Fig. 2). A methodology was also developed to rank piers for deterioration based on data from UAS inspections. The author believes this is one of the largest deployments of NDE technologies through these platforms to date.

The UAS was a Skydio X10 drone equipped with artificial intelligence (AI) technology to focus sensors where needed (Fig. 2). This system is capable of being airborne in less than 40 seconds, and it can navigate autonomously during the night. A wireless link between the UAS and its controller allows control over line-of-sight distances of up to 7.5 miles (12 km). The UAS is 31.1 x 25.6 x 5.7 in. (790 x 650 x 145 mm). Including batteries, the device weighs 4.65 lb (2.11 kg), and its maximum takeoff weight is 5.49 lb (2.49 kg). Its maximum horizontal speed is 45 mph (72.4 km/h), and it can withstand wind gusts of 28 mi/hr (12.8 m/s). The drone's maximum flight time is 40 minutes.

The crawling robot was a HausBots HB2 (Fig. 2). This robot uses Aerogrip™ technology, a suction and airflow hybrid that allows for high downforce of about 78.7 lb (350 N) to keep it attached to a vertical surface. The robot requires about 1800W to operate, and this power is supplied by a tether cable. With a 76.25 ft (25 m) tether, the robot's payload capacity is 8.81 lb (4 kg).

NDE technologies

The UAS was mounted with HRI and IR cameras, and the crawling robot was mounted with GPR and an HRI camera. Manual NDE of the piers was conducted using GPR, ultrasonic pulse echo, ultrasonic pulse velocity, and electrical resistivity. However, due to space limitations, only GPR results in the manual NDE are presented and discussed herein. The deployments of the NDE technologies were accomplished using a boat to transport the crew to the piers, navigate from one pier to another, and serve as a work platform for testing the piers.

Pier deterioration ranking methodology

The UAS survey with HRI and IR cameras generated a large amount of data, with more than 107,000 image files. Given this vast amount of data, it was not practical to manually quantify surface damage in each of the 36 piers and then identify the 10 piers with the most deterioration. A quantitative procedure was developed to rank the piers according to the extent of damage relative to each pier's total surface area. Two types of rankings were developed: one based on identified cracks and the other based on surface defects, including cracks, spalls, and exposed corroded reinforcing steel. In this procedure, images of a pier were examined to ensure that each instance of damage appeared in only one image. Then the damage was marked using image annotation software ROBOFLOW (Fig. 3 and 4). The total number of damage pixels in each image was then calculated, using a program coded in Python. Finally, the damage ratio for each pier was calculated to establish a deterioration ranking. Based on all the surface defects, 10 piers were selected for detailed investigation: Piers 5, 11, 16, 20, 22, 24, 26, 30, 31, and 36.

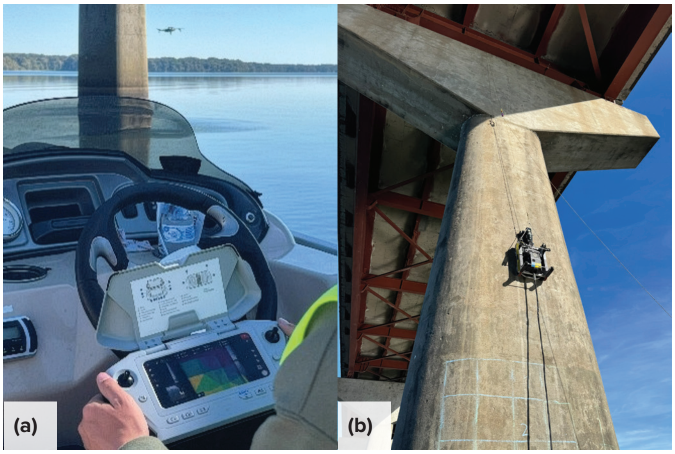

Fig. 2: Systems used in this study: (a) a pilot on a boat uses a controller to maneuver the UAS near the pier in the background; (b) the crawling robot moves along the pier shaft

Fig. 3: Images of Pier 5 were captured using the UAS and subsequently annotated to highlight surface defects

Fig. 4: Enhanced UAS-captured images of Pier 30

Although only HRI was used to rank the piers' deterioration, IR images were used to confirm the defects identified by HRI. Despite the limitations the IR thermography technique has, for example, sunny or overcast conditions and the piers being under the shadow of the deck, the defects identified by the two techniques were consistent. Figure 5 shows a specific area of Pier 30 where a fine crack can be seen in both the HRI and IR images. Also, the IR image shows the likelihood of some subsurface deterioration adjacent to the crack, as evidenced by warm colors.

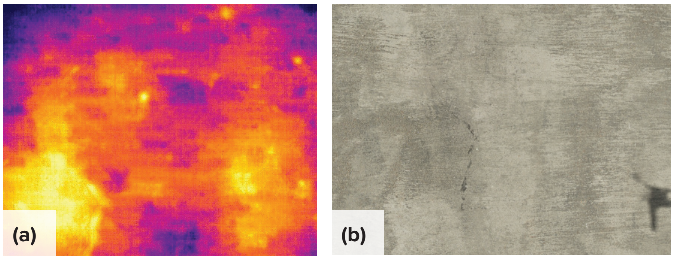

Fig. 5: A specific area of Pier 30 with a crack: (a) IR image; and (b) HRI image

Results and Discussion

The results of the robotic and manual NDE are described in the following sections.

Robotic NDE

A 10 x 10 ft (3.05 x 3.05 m) area of each pier was examined using the crawling robot. At each pier, 10 GPR scans were conducted at 1 ft (0.3 m) vertical spacing. All GPR

Table 1:
Concrete cover and reinforcing steel spacing on the southwest face of Pier 30

Scan No.	Maximum reinforcing steel depth (in.)	Minimum reinforcing steel depth (in.)	Average reinforcing steel depth (in.)	Reinforcing steel spacing (in.)
1	6.60	5.80	6.20	23.16
2	6.80	5.80	6.30	23.76
3	7.90	6.50	7.20	24.20
4	9.00	6.90	7.95	23.50
5	8.60	7.10	7.85	24.50
6	6.30	5.70	6.00	23.70
7	5.60	5.00	5.30	23.00
8	4.40	3.90	4.15	24.00
9	3.60	3.40	3.50	23.00
10	2.90	2.50	2.70	22.60

Note: 1 in. = 25 mm.

scans were performed on the southwest face of the piers, except for Pier 36, which is located onshore. The scans of this pier were taken from the northeast face of the pier.

In the analysis of GPR signals, the top steel reflection technique was used where the reflection amplitudes from the scan nearest to reinforcing steel detected in the data are compared with the reflection amplitudes recorded at other locations. In this technique, the amplitude of reflections along a radar pass provides an indication of the concrete's condition; the lower the amplitude of reflections, the higher the likelihood of deterioration.

A detailed analysis of the depth of concrete cover over reinforcing steel (minimum, maximum, and average) and spacing between reinforcing steel performed for Pier 30 for all the GPR scans made on this pier is provided in Table 1.

From Table 1, it can be noted that the average concrete cover from all 10 scans is 6.1 in. (155 mm), and the average reinforcing steel spacing is 23.7 in. (602 mm). The reinforcing steel spacing of 23.7 in. compares well with the transverse bar spacing of 24 in. (610 mm) measured in a limited GPR testing conducted on the piers in 2018 by others. Also, an average concrete cover of 6.1 in. compares well with the concrete cover for transverse bars (stirrups) in the plans for Pier 30, which is 5.7 in.

The vertical line scanning GPR results for all 10 scans of Pier 30 are shown in Fig. 6 as a deterioration map. For comparison, the deterioration maps for Pier 30 that were tested manually are also presented here. In these deterioration maps, red represents a high likelihood of deterioration, while green represents a low likelihood of deterioration. Yellow falls between these two bands and represents a moderate likelihood of deterioration.

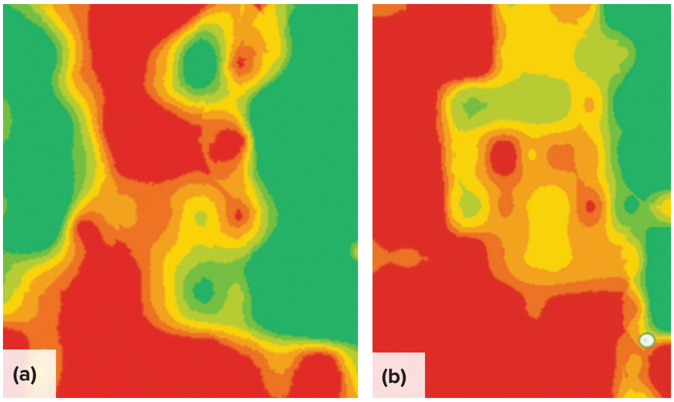

Fig. 6: Deterioration map for the southwest face of Pier 30: (a) robotic NDE; and (b) manual NDE

Manual NDE

Manual NDE of the piers was performed to compare with the findings of the UAS and robotic NDE. In the manual NDE, testing was performed on both faces of the piers, and, depending on the size and shape of piers, either 6 x 8 ft (1.83 x 2.44 m) or 7 x 7 ft (2.13 x 2.13 m) areas centered on both faces of each pier were tested at a grid of 1 x 1 ft. A total test area of about 100 ft^2 (9.3 m^2) was covered for each of the 10 piers. The GPR scans were made along the horizontal gridlines, rather than the vertical gridlines inspected using the robot.

Significant variation in the likelihood of deterioration estimated was observed using the robotic NDE and manual NDE. For Pier 30, for example, the likelihood of deterioration estimated by robotic NDE is 54%, and that by manual NDE is 80% (Fig. 7). There are several reasons for this variation. The primary reason is that the robotic NDE was conducted vertically, and the manual GPR testing was conducted horizontally. The deterioration maps developed from robotic NDE data are based on reflections from horizontal reinforcing bars spaced at 24 in., whereas the maps developed from manual GPR testing are based on reflections from longitudinal reinforcing bars spaced at 12 in. (304.8 mm). Robotic and manual surveys were not conducted on the same gridlines. The grids in the manual testing program were either 6 x 8 ft or

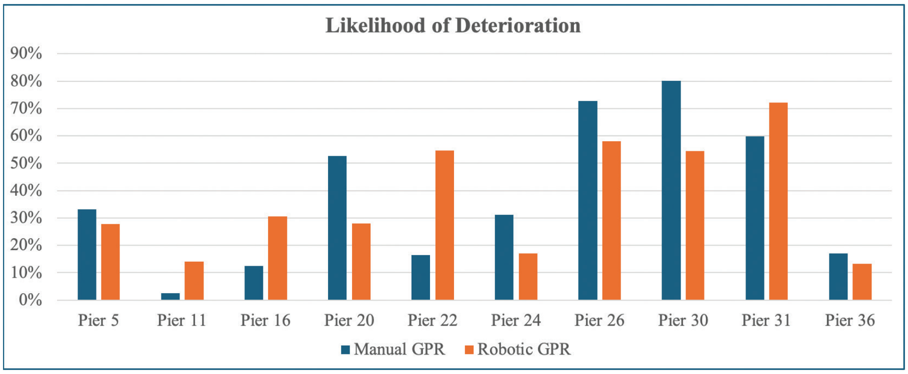

Fig. 7: Estimated areas of probable subsurface deterioration based on manual and robotic GPR inspections

Fig. 8: Core taken from the southwest face of Pier 30

7 x 7 ft on each face of the pier, for a total test area of 100 ft^2. The grids in the robotic testing program covered the entire test area of 100 ft^2 over only one face of the pier (the southwest face, except for Pier 36). Thus, although both systems were used to inspect the same general vicinity on one face of each pier, the robotic inspection covered twice the area covered by manual inspection. Further, the 1 ft spacing and variance in the paths of the inspection scans for the two systems likely allowed some defects to be missed by both or one of the systems. While it would have been ideal to conduct both the manual and robotic GPR testing horizontally along the same gridlines, the crawling robot can only climb—it was not possible to conduct robot inspections along horizontal paths.

Despite differences in the location of test grids and direction of scans between the robotic and manual GPR testing programs, some comparability is expected between the two in terms of total estimated suspect subsurface deterioration areas (Fig. 7).

In Fig. 7, it can be noted that piers with a low level of deterioration are low in both testing programs. Similarly, piers with a high level of deterioration are high in both testing programs.

Validation of NDE results

Cores were retrieved from five of the 10 piers tested, including Piers 5, 11, 24, 30, and 36. The locations of the five retrieved cores and their conditions validate the NDE test results. Results for Pier 30 are discussed in the following. The subsurface deterioration area on the southwest face of this pier was estimated to be 80 and 54% by the manual GPR testing program and the robotic GPR testing program, respectively (Fig. 7).

The location of the core is indicated as a white circle on the manual GPR deterioration map of the pier (refer to Fig. 6). This pier had a large network of cracks exceeding 0.05 in. (1.27 mm) in width. Crack depths of up to 4.65 in. (118.1 mm) were measured by ultrasonic pulse velocity testing. As shown in Fig. 8, the core was retrieved from one of these crack locations.

This core has multiple cracks, with the surface crack at which the core was taken extending to about 3 in. (76.2 mm) from the surface. There were also two major horizontal cracks at different depths of the core, and it almost broke apart. Visual inspection also showed that the core contained reacted and cracked aggregates. The condition of the core is consistent with the NDE testing results.

Conclusions

The study's objectives included demonstrating the effectiveness of using a uncrewed aerial systems (UAS) and a crawling robot for bridge pier inspection and testing in a real-world setting. This objective was successfully achieved. While the John Coffee Memorial Bridge presented a challenging setting, the platforms for the deployment of nondestructive evaluation (NDE) technologies were shown to substantially reduce the time required for inspection. Accordingly, they reduced costs and improved the safety of personnel involved in the testing as well as the traveling public (which is impacted by traffic control). In addition to being used to identify surface defects on the bridge's piers, the images captured using the UAS-mounted cameras were used to generate three-dimensional (3-D) models of the piers—this would not be possible using conventional visual inspection.

This study has demonstrated the utility and effectiveness of the crawling robot for bridge inspection and testing, particularly on vertical surfaces. The study also provided an opportunity for a one-to-one comparison of the robotic NDE and manual NDE. Acknowledging that more NDE technologies were used in the manual NDE program than in the robotic NDE program, the personnel time required in manual NDE was much greater than in robotic NDE. In the manual NDE program, a crew of four to five, excluding the two boat operators, was fully engaged for 2 weeks to complete the testing. In the robotic NDE program, a three-person crew completed testing in 1 week, despite weather challenges on a few days. Further, the manual NDE could reach a maximum height of only 10 ft above water. And that was a stretch, because it required the use of a stepstool placed on the boat to reach the topmost gridline. This would have posed safety concerns if the river's water currents were not as stable as they were at the time of the manual NDE program. On the other hand, the crawling robot could have reached the full height of the pier, starting from the level of the boat to the top edge of the pier cap (although the robot would not have been able to reach the cap's projecting extensions). And, finally, if manual NDE was to be done from the bottom to the top of the pier, a snooper truck on the deck, traffic control for the snooper truck, and a bucket boat over the river waters would have been needed, as noted in the 2018 study mentioned earlier.

The maneuverability of the crawling robot is currently limited to a vertical path that needs to be the same for the climbing and return of the robot. The robot cannot take a right turn, left turn, or U-turn like a drone or automobile. Further developments will make the crawling robot even more useful and effective than it is today.

From the UAS survey, the condition of the piers above water appears to be fair, which is consistent with data gathered during the bridge's biennial safety inspections. The bridge has consistently received a National Bridge Inspection Standards (NBIS) condition rating of 6. However, the NDE and cores retrieved from these piers show that several of the tested piers are in poor condition. This study demonstrates that surface inspections alone are not sufficient to assess the condition of bridge elements and highlights the importance of using NDE systems that can detect subsurface deterioration and defects.

Acknowledgments

The investigation presented in this paper was funded by the U.S. Federal Highway Administration (FHWA). The publication of this paper does not necessarily indicate approval or endorsement of the findings, opinions, conclusions, or recommendations, either inferred or specifically expressed herein, by the FHWA or the U.S. Government.

References

1. Zink, J., and Lovelace, B., "Unmanned Aerial Vehicle Bridge Inspection Demonstration Project," Report No. MN/RC 2015-40, Minnesota Department of Transportation, St. Paul, MN, July 2015, https://mdl.mndot.gov/_flysystem/fedora/2023-01/201540.pdf.

2. Wells, J., and Lovelace, B., "Unmanned Aircraft System Bridge Inspection Demonstration Project Phase II," Report No. MN/RC 2017-18, Minnesota Department of Transportation, St. Paul, MN, June 2017, https://transportation.org/uas-aam/wp-content/uploads/sites/80/2023/05/201718.pdf.

3. Quinton, D. Regan, T., "Use of Unmanned Aerial Systems (UAS) by State DOTs," Report No. FHWA-HIF-18-060, American Association of State Highway and Transportation Officials, Washington, DC, Nov. 2018, https://www.fhwa.dot.gov/uas/peer/2018peer.pdf.

4. Khan, M.S., "Bridge Management Systems: Past, Present, and Future," *Concrete International*, V. 22, No. 8, Aug. 2000, pp. 53-56.

5. NCHRP Report Synthesis 501, "Pavement Management Systems: Putting Data to Work," K.A. Zimmerman, ed., Transportation Research Board and National Academies of Sciences, Engineering, and Medicine, The National Academies Press, Washington, DC, 2017. doi: 10.17226/24682

6. Gucunski, N.; Basily, B.; Kim, J.; Yi, J.; Duong, T.; Dinh, K.; Kee, S.-H.; and Maher, A., "RABIT: Implementation, Performance Validation and Integration With Other Robotic Platforms for Improved Management of Bridge Decks," *International Journal of Intelligent Robotics and Applications*, V. 1, 2017, pp. 271-286. doi: 10.1007/s41315-017-0027-5

7. Bigman, D.P., "Evaluating the Feasibility of Robotic Crawler Deployed Ground Penetrating Radar to Assess Repairs of a Concrete Hydroelectric Dam Spillway in Alabama, USA," *Water*, V. 15, No. 10, May 2023. doi: 10.3390/w15101858

8. Shams, S.; Ghorbanpoor, A.; Lin, S.; and Azari, H., "Nondestructive Testing of Steel Corrosion in Prestressed Concrete Structures Using the Magnetic Flux Leakage System," *Transportation Research Record: Journal of the Transportation Research Board*, V. 2672, No. 41, 2018, pp. 132-144. 036119811877392. doi: 10.1177/0361198118773920

Selected for reader interest by the editors.

Mohammad S. Khan, FACI, is an Executive Vice President at HPTech. Prior to joining HPTech in 2017, he was a Senior Vice President with Intertek-PSI. Khan has more than 30 years of experience in engineering research, and testing and evaluation of structures, particularly bridges. He is a past Chair and current member of ACI Committees 123, Research and Current Developments; 222, Corrosion of Metals in Concrete; and 357, Offshore and Marine Concrete Structures; and a member of ACI Committee 201, Durability of Concrete. Khan received his PhD in civil engineering from Oklahoma State University, Stillwater, OK, USA, in 1992.